Published in IET Microwaves, Antennas & Propagation
Received on 7th November 2006
Revised on 27th November 2007
doi: 10.1049/iet-map:20060305

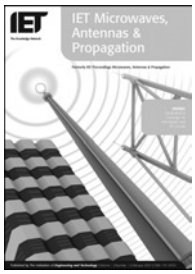

ISSN 1751-8725

Hybrid channel modelling for ultra-wideband portable multimedia applications

K.M. Nasr

BBC Research, British Broadcasting Corporation, Kingswood Warren, Surrey KT20 6NP, United Kingdom
E-mail: karim.nasr@bbc.co.uk

Abstract: An efficient approach in modelling the ultra-wideband channel (UWB) by combining deterministic and statistic techniques is presented. The hybrid approach aims at lowering the complexity of modelling the UWB indoor channel by combining simple 2.5D ray tracing and measurement statistics. A UWB measurement campaign in an office environment is reported. The mean signal level and the rms delay spread values obtained from the ray-tracing tool are compared with measurements at several locations in the studied environment. Average statistical difference terms are added to the values of mean signal level and rms delay spread obtained from ray tracing to improve predictions. This approach results in the hybrid model and achieves computational efficiency by eliminating the need of modelling complex details of scatterers in the environment.

1 Introduction

There is currently a considerable interest in ultra-wideband (UWB) and wireless personal networks systems as a solution for the high capacity problem of short-range indoor wireless applications, which has led to the change in regulations to allow UWB communications [1–3].

UWB systems rely generally on very short noise like pulses that can achieve a high data transfer rate by operating over a large bandwidth. UWB devices typically operate in the range of 3.1–10.6 GHz with a bandwidth of at least 500 MHz. There is a wide range of applications exploiting UWB technology including ground penetrating radars, through-wall imaging, collision avoidance (vehicular) radar, medical imaging, short-range indoor wireless communications and others. An example of the above applications is short-range ($<$10 m) indoor wireless communications (e.g. a universal serial bus device [4]). Our target application is a UWB portable device that enables large multimedia files to be accessed and exchanged with an infrastructure network at high rates through the air.

To build UWB systems, it is crucial to understand and model the UWB propagation channel efficiently and to a good accuracy.

The main approaches used to model the UWB channel rely either on statistical (empirical) modelling as in [5–7] or deterministic modelling. Deterministic modelling is normally based on ray tracing or finite difference time domain (FDTD) [8, 9]. Standardisation efforts such as IEEE 802.15.3a for short-range applications and IEEE 802.15.4a aim at modelling the UWB channel in different scenarios with a variety of ranges for system evaluation purposes [10, 11].

The main problem with deterministic modelling based on ray tracing is the computation complexity which grows exponentially as the number of scatters and details in the environment (e.g. furniture) are included. The other important issue is how to include frequency-dependent material parameters for UWB. Statistical modelling cannot be generally applied except to environments that are similar to the measured environment that was used to collect the statistics.

The target of this paper is twofold: first to report the results of a UWB measurement campaign in an office environment and secondly to present an efficient hybrid approach for UWB channel modelling. This approach relies on using 2.5D ray tracing with material parameters (dielectric constant and conductivity) evaluated as an average of the value of the parameters within the wide frequency range. The wideband ray-tracing predictions are then combined with statistical differences obtained from measurements. This eliminates the need of using a sophisticated ray tracer that would take into account the details of furniture or small scatterers. The hybrid model results in a simple yet efficient way to model the UWB indoor channel.

Previous work combining statistical and deterministic modelling for UWB [5, 12] concentrated on modelling the clusters of diffuse multipath components as a statistical distribution that is added to the main dominant echoes. The target of the hybrid model of this paper is different and is namely a simple and fast approach for the estimation of UWB coverage (local field strength values) within an environment as well as the rms delay spread values.

The paper is organised as follows: In Section 2, the UWB measurement campaign is described. Section 3 compares the predictions from ray tracing and measurements and Section 4 presents the hybrid model. Section 5 concludes the paper.

2 Measurement campaign

The measurements were taken within the premises of a typical modern office environment using a vector network analyzer. The frequency sweep was setup from 2 to 6 GHz with a total bandwidth of 4 GHz with 801 points corresponding to a 5 MHz frequency step. A calibration process was done to the measuring equipment to remove the effect of cables and other hardware on the measured channel impulse responses. Wideband discone antennas were used with nearly omnidirectional characteristics in the azimuth plane. The transmitter and receiver antennas were kept at the same height of ~90 cm. Hamming windowing was applied to the measured data because of its good sidelobe suppression characteristics [13]. An inverse fast Fourier transform was used to obtain the channel impulse responses from the measured frequency transfer functions.

Nine measurements were recorded on a grid pattern at every location and averaged. The grid points were separated by $<\lambda/2$ at the highest frequency (6 GHz), that is, (2–2.5 cm). An illustration of the grid pattern is shown within Fig. 1 next to Rx1

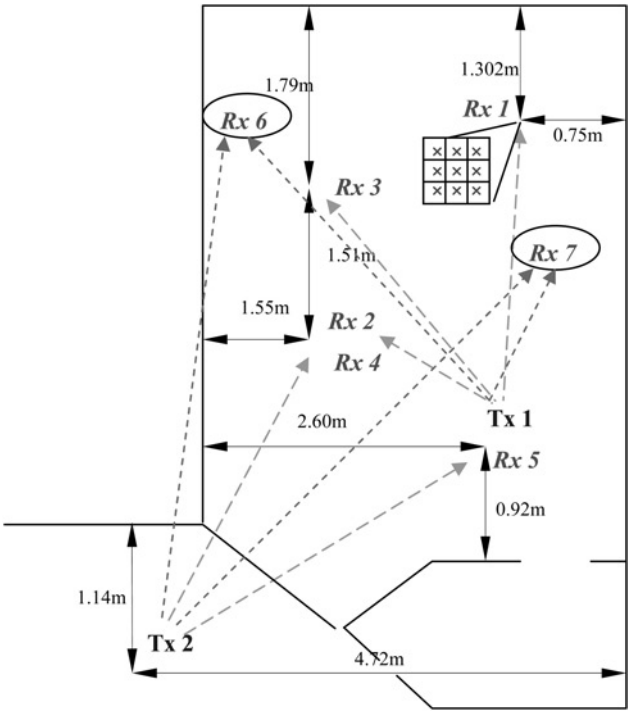

Figure 1 *Details of the measurement locations showing the positions of the transmitters, the receivers and the grid of measurements*

A layout of the office environment is shown in Fig. 1 with some of the locations of transmitters and receivers highlighted. Fig. 2 shows the measurement equipment used and the antennas relative positions inside a room for one of the measurement locations. Fig. 3 shows the wideband discone antenna used in the measurements and its average patterns (over the 4 GHz bandwidth) in azimuth and elevation.

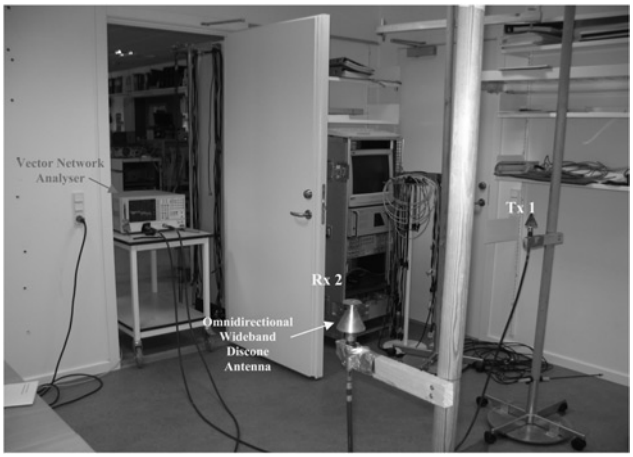

Figure 2 *LOS position Tx1–Rx2 showing the measuring equipment used and the antennas*

a Discone antenna with height and diameter of ~5 cm each
b Average azimuth pattern
c Average elevation pattern

doi: 10.1049/iet-map:20060305

Two particular scenarios were investigated for the target application: (a) communication within a room (e.g. Tx1 to Rx1 to 4) and communication where the UWB transmitter is in the corridor and the receiver is obstructed in the room (e.g. Tx2 to Rx2, 4 and 5). These scenarios were selected since they are likely to occur in practice for the target application where a user exchanges large multimedia files between a portable UWB device and a computer.

3 Ray-tracing modelling against measurements

A ray-tracing tool [14, 15] is used to predict the signal level at the receiver positions of Fig. 1. The 2.5D ray-tracing model for an arbitrary indoor architecture and wall properties was simulated based on the method of images. The model accounts for the line-of-sight (LOS) path, multiple reflections, diffractions from corners and transmission loss through walls. The first step is the definition of the studied architecture. The way of inputting the studied architecture database affects the computation time. If two walls (objects) are on the same line and share the same electromagnetic properties, they are defined as a single object. This simple and careful procedure in inputting the database can greatly reduce the number of objects and hence the calculation time.

After defining the arbitrary geometry in terms of points (lines) and arbitrary electromagnetic material properties (permittivity and conductivity), the LOS path angles and transmission loss [if any intersecting walls (objects) are present] are calculated. The main procedure used for ray tracing is to successively project the transmitter(s) on all the walls to obtain first and second (or more generally higher) order images, and then to determine the valid intersection points on the walls. Once valid intersection points on the walls are determined (i.e. lying on the wall and not outside), the valid rays are identified and the angles with the normal to the walls are calculated.

The electromagnetic properties for common building materials at 2.4 and 5.8 GHz [16–18] are used to calculate the average reflection and transmission coefficients for a transverse electromagnetic (TEM) wave with perpendicular polarisation within the ultra wideband extending from 2 to 6 GHz and used in measurements. Table 1 summarises the average permittivity and conductivity values of some building materials used in the ray-tracing simulations. The frequency of operation for ray-tracing simulations is selected in the middle of the measurement band (i.e. at 4 GHz) and the wavelength λ is hence 7.5 cm.

The effective transmission loss for all the walls is obtained by multiplying the individual transmission

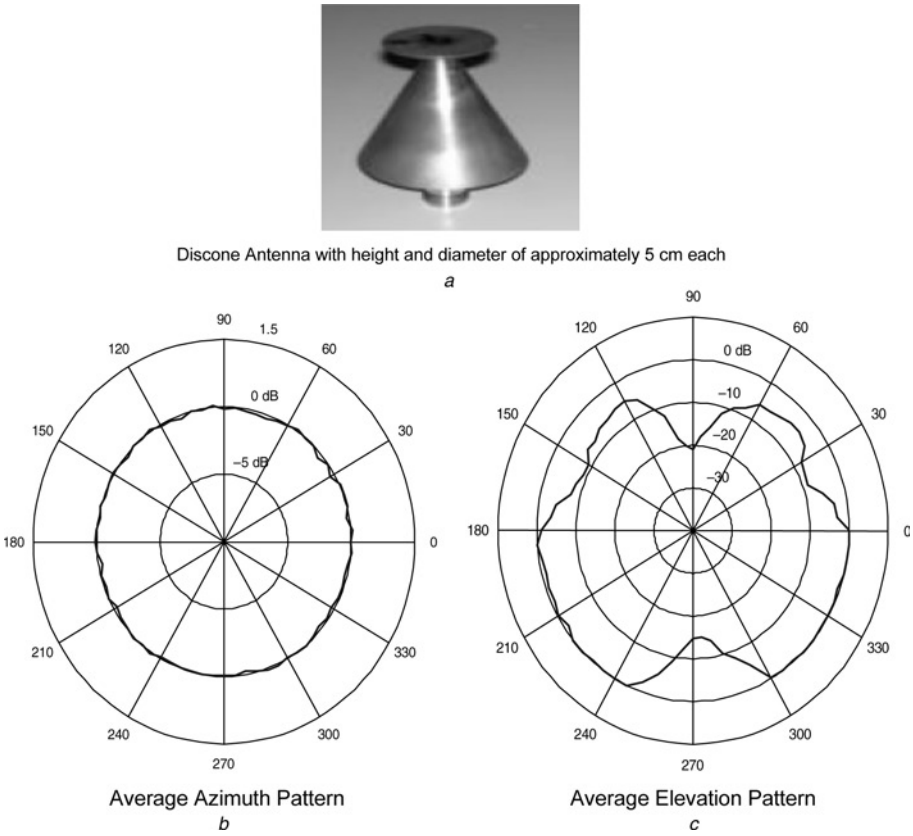

Figure 3 *Wideband discone antenna and its average azimuth and elevation patterns from 2 to 6 GHz*

doi: 10.1049/iet-map:20060305

Table 1 Summary of average electromagnetic properties values of some building materials used in the ray-tracing simulations

Material	Relative permittivity ε_{real}	Conductivity, σ (S/m)
concrete	4.85	0.173
brick wall	3.92	0.0648
doors	5.21	0.055
plaster board	2.18	0.01
chipwood	2.6	0.1
glass	5.05	0.3

loss of every contributing wall and similarly for the effective reflection loss. The complex received electric field E_{rp} associated with the pth ray is determined by

$$E_{r_p} = E_{oref} A_{\theta,\varphi} \prod_{wr} R_{ep,eh} \prod_{wt} T_{cep,eh} \frac{e^{-j\beta d_p}}{d_p} \quad (1)$$

where E_{oref} is the reference field strength, wr is to account for all existing reflection coefficients from wr contributing walls, wt is to account for all transmission coefficients from wt contributing walls, d_p the unfolded ray path length to account for the path loss, β the propagation constant, $R_{ep,eh}$ the reflection coefficient that takes into account the polarisation and thickness of the wall [19] and the transmission coefficient $T_{cep,eh}$ is calculated based on the following equation [20]

$$T_{c_{ep,eh}} = \sqrt{\chi(1 - \left|R_{ep,eh}\right|^2)} \quad (2)$$

where χ is a coefficient that accounts for losses because of diffuse scattering and is normally taken as 0.5. The term $A_{\theta,\phi}$ takes into account the effect of the antenna pattern in the azimuth and elevation planes.

Diffraction from corners is simulated by modelling the corner as an absorbing screen [21].

If any of the calculated diffracted paths are obstructed, the transmission loss is taken into account as before which further reduces the diffracted field strength. Approximating a curve into a series of lines can simulate curved surfaces in the architecture. The 2.5D tool implements first the processing of the plane followed by the elevation of the architecture and finally averaging the results.

The rms delay spread τ_{rms} is defined as the square root of the second central moment of the power delay profile (PDP) and quantifies the time dispersion of the studied environment. It can be determined from the obtained PDP according to the following equations [22, 23]

$$\tau_{rms} = \sqrt{\overline{\tau^2} - (\overline{\tau})^2} \quad (3)$$

The mean excess delay is the first central moment of the PDP and is defined as

$$\overline{\tau} = \frac{\sum_p (A_p)^2 \tau_p}{\sum_p (A_p)^2} \quad (4)$$

$$\overline{\tau^2} = \frac{\sum_p (A_p)^2 \tau_p^2}{\sum_p (A_p)^2} \quad (5)$$

A_p is defined as the amplitude of the field of path p.

The average received signal strength at a particular location is calculated using the spatial sampling approach by averaging the block of points of $(5\lambda \times 5\lambda)$ or the more computation efficient wall imperfection model as in [14].

An example of the ray-tracing simulations for position (Tx1, Rx1) of Fig. 1 is presented in Fig. 4 showing the power delay angular profile. The measured average PDP for the same position is shown in Fig. 5 (averaged over a block of nine measurement points both in plane and elevation).

The ray-tracing simulations take into account the whole floor plane of the building to further improve the accuracy especially for the rms delay spread values. The direction of arrival and departure are also identified and used to apply the antenna pattern effect at the two end of the link.

doi: 10.1049/iet-map:20060305

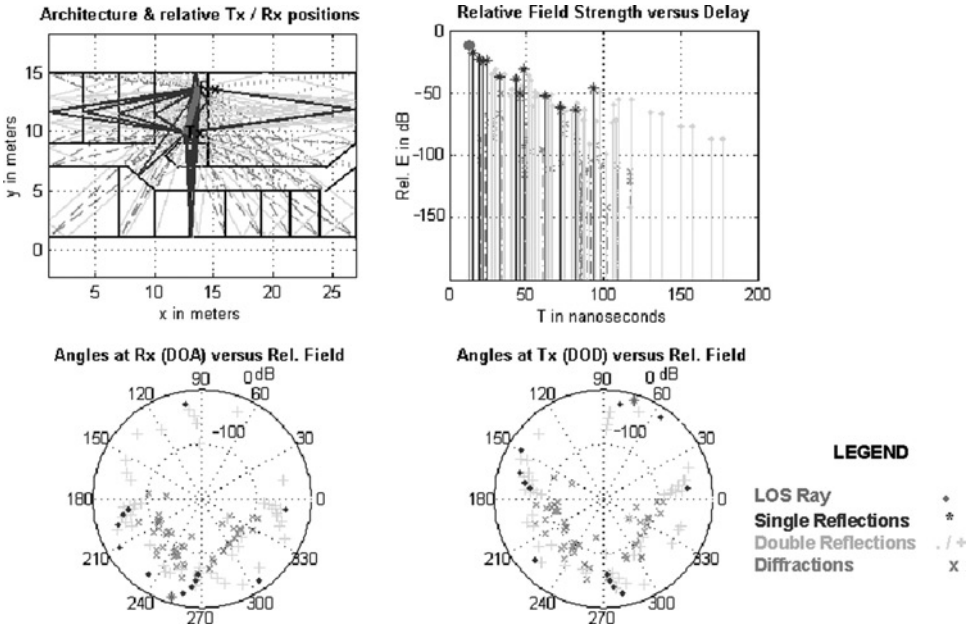

Figure 4 *Ray-tracing simulation output for position (Tx1, Rx1) taking into account the rest of the floor plane*

Comparisons between the predicted field strength and rms delay spread values from the ray-tracing tool after averaging a block of points using the spatial sampling approach [14] and averaged measurements at the different positions of Fig. 2 are summarised in Table 2. It is concluded that the ray-tracing tool predicts the field levels higher than actual measurements with an average difference of 6.68 dB and predicted the rms delay spread values lower than measurements with an average difference of 7.21 ns.

4 Hybrid channel model

As would be expected with any channel modelling tool, differences will occur with measurements and the target is to minimise this difference without increasing the complexity of the model (such as modelling furniture, small scatterers or resorting to a more time consuming and complex 3D tool) to achieve computation efficiency. Based on the above comparisons of Table 2, it is possible to add an empirical term to the ray-tracing prediction resulting in the following hybrid model

$$E_{\text{hyb}} = E_{\text{RT(avg)}} + E_{\text{stat}}(\text{dB}) \tag{6}$$

where E_{hyb} is the average predicted field strength from the hybrid model, $E_{\text{RT(avg)}}$ the average predicted field strength from the ray-tracing tool in decibel and E_{stat} the additional empirical field strength difference term from measurement statistics and in the above case is equal to −6.68 dB.

Similarly for the rms delay spread

$$\tau_{\text{hyb}} = \tau_{\text{RT}} + \tau_{\text{stat}}(\text{ns}) \tag{7}$$

where τ_{hyb} is the predicted rms delay spread from the hybrid model, τ_{RT} the average predicted rms delay spread value from the ray-tracing tool in nanosecond and τ_{stat} the additional empirical rms delay spread difference term from measurement statistics and in the above case is equal to 7.21 ns.

Using the above hybrid model, the error in prediction reduces to a fraction of a decibel for average field strength value and around 1 ns for the rms delay spread value in the worst cases.

The tool can then be used to investigate other points within the architecture or other similar architectures and positions within the building under study and form a coverage map and a distribution of delay spread values without the need of a costly and

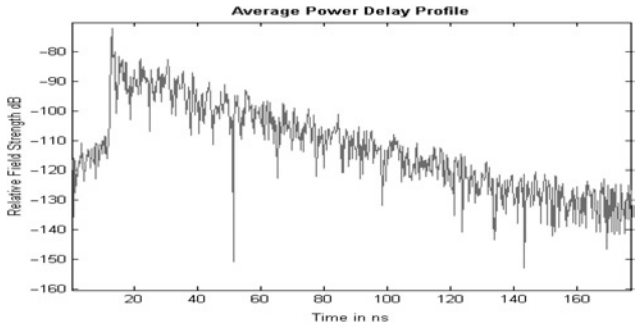

Figure 5 *Measured average PDP for position (Tx1, Rx1)*

doi: 10.1049/iet-map:20060305

Table 2 Comparisons of measured and predicted average field strength and rms delay spread values at the different locations of Fig. 1

Location	Measured field strength, dB	Predicted field strength, dB	Difference, dB	Measured rms delay spread, ns	Predicted rms delay spread, ns	Difference, ns
Tx1–Rx1	−76.93	−70.01	6.92	12.73	6.68	6.05
Tx1–Rx2	−75.87	−69.82	6.05	12.65	4.38	8.27
Tx1–Rx3	−74.70	−68.46	6.24	11.75	3.91	7.84
Tx2–Rx4	−94.36	−87.21	7.15	17.32	9.87	7.45
Tx2–Rx5	−93.29	−86.23	7.06	16.10	9.63	6.47
Average difference			6.68			7.21

Table 3 Comparisons of measured and predicted hybrid model value at the new locations of Fig. 1

Location	Measured field strength, dB	Predicted field strength, dB	Difference, dB	Measured rms delay spread, ns	Predicted rms delay spread, ns	Difference, ns
Tx1–Rx6	−78.53	−77.71	0.82	13.15	12.08	1.07
Tx1–Rx7	−76.08	−75.62	0.46	11.93	11.21	0.72
Tx2–Rx6	−02.24	−01.12	1.12	19.77	18.01	0.76
Tx2–Rx7	−98.36	−97.51	0.85	18.52	17.38	1.14
Average difference			0.81			0.92

time-consuming measurement campaign. Other possible uses of the hybrid tool are coexistence studies (e.g. to model and estimate the interference of a number of UWB transceivers to a wireless local area network (WLAN) system).

To further validate the hybrid model, new locations Rx6 and Rx7 of Fig.1 are measured and compared with the predictions from the hybrid model. The results are summarised in Table 3. It is concluded that the average error in the field strength prediction is now 0.81 dB, whereas the average error in the rms delay spread is 0.92 ns as would be expected.

5 Conclusions

This paper presented an efficient approach to model the UWB indoor radio channel based on combining deterministic and statistical results. This approach has the advantage of lowering the computation complexity and time (by removing the need to model complex scatterers like furniture details) for the prediction of average field strength or coverage of a UWB transceiver as well as rms delay spread values at arbitrary locations within an environment of interest. Results of a UWB measurement campaign in a typical office environment were reported targeting short-range high data-rate UWB multimedia applications. The presented approach is based on combining the deterministic modelling relying on 2.5D ray tracing and average statistical differences retrieved from measurements. It was shown that the prediction error reduces considerably by using the hybrid model. For the example office environment studied, errors in the average predicted field strength using the hybrid approach are lower than a decibel compared with measurements. Similarly, the errors for rms delay spread values are around 1 ns.

6 Acknowledgments

Thanks are due to European COST Action 273: 'Towards Mobile Broadband Multimedia Networks' for sponsoring the UWB measurement campaign and to Prof. Jørgen Bach Andersen and his research group at the Antennas and Propagation Division, Department of Communication Technology of Aalborg University in Denmark for hosting Dr. Karim Nasr and for their willing assistance with the measurements.

doi: 10.1049/iet-map:20060305

7 References

[1] Federal Communications Commission, FCC rules section 15.517, available at: www.fcc.gov

[2] WIN M.Z., SCHOLTZ R.A.: 'Impulse radio: how it works', *IEEE Commun. Lett.*, 1998, **2**, (2), pp. 36–38

[3] SIWIAK K.: 'Ultra wide band radio: introducing a new technology'. IEEE 53rd Vehicular Technology Conf. VTC2001, 2001, vol. 2, pp. 1088–1093

[4] Intel White Paper Wireless USB: 'The first high speed personal wireless interconnect', available at: www.intel.com/technology/ultrawideband2004

[5] SALEH A.M., VALENZUELA R.A.: 'A statistical model for indoor multipath propagation', *IEEE J. Sel. Areas Commun.*, 1987, **5**, (2), pp. 128–137

[6] CASSIOLI D., WIN M.Z., MOLISCH A.F.: 'The ultra-wide bandwidth indoor channel: from statistical model to simulations', *IEEE J. Sel. Areas Commun.*, 2002, **20**, (6), pp. 1247–1257

[7] GHASSEMZADEH S.S., JANA R,, RICE C.W., TURIN W,, TAROKH V.: 'Measurement and modeling of an ultra-wide bandwidth indoor channel', *IEEE Trans. Commun.*, 2004, **52**, pp. 1786–1796

[8] BROWN A.K.: 'Ultrawideband propagation–an overview', The IEE Seminar on Ultrawideband Communications Technologies and System Design, July 2004, pp. 31–34

[9] MOLISCH A.F.: 'Ultrawideband propagation channels—theory, measurement, and modeling', *IEEE Trans. Veh. Technol.*, 2005, **54**, (5), pp. 1528–1545

[10] WPAN High Rate Alternative PHY. IEEE 802.15.3a Task Group 2005 [Online]. Available at: http://www.ieee802.org/15/pub/TG3a.html

[11] WPAN Low Rate Alternative PHY. IEEE 802.15.4a Task Group 2005 [Online]. Available at: http://www.ieee802.org/15/pub/TG4a.html

[12] KUNISCH J., PAMP J.: 'Measurement results and modeling aspects for the UWB radio channel'. IEEE Conf. Ultra Wideband Systems and Technologies, May 2002, pp. 21–29

[13] OPPENHEIM A.V., SCHAFER R.W.: 'Discrete-time signal processing' (Prentice-Hall, Upper Saddle River, NJ, 1999, 2nd edn.)

[14] NASR K.M., COSTEN F., BARTON S.K.: 'A wall imperfection channel model for signal level prediction and its impact on smart antenna systems for indoor infrastructure WLAN', *IEEE Trans. Antennas Propag.*, 2005, **AP-53**, (11), pp. 3767–3775

[15] NASR K.M., COSTEN F., BARTON S.K.: 'A spatial channel model and a beamformer for smart antennas in broadcasting studios'. 12th Int. Conf. Antennas and Propagation (ICAP 2003), March 2003, vol. 2, pp. 828–831

[16] CUINAS I., SANCHEZ M.G.: 'Measuring, modelling and characterizing of indoor radio channel at 5.8 GHz', *IEEE Trans. Veh. Technol.*, 2001, **50**, (2), pp. 526–535

[17] ANDERSON C.R., RAPPAPORT T.S.: 'In-building wideband partition loss measurements at 2.5 and 60 GHz', *IEEE Trans. Wirel. Commun.*, 2004, **3**, (3), pp. 922–928

[18] STAVROU S., SAUDERS S.R.: 'Review of constitutive parameters of building materials'. 12th Int. Conf. Antennas and Propagation (ICAP 2003), March 2003, vol. 1, pp. 211–215

[19] CATEDRA M.F., PEREZ-ARRIAGA J.: 'Cell planning for wireless communications' (Artech House, 1999)

[20] BERTONI H.L., HONCHARENKO W., MACIEL XIA H.H.: 'UHF propagation prediction for wireless personal communications', *Proc. IEEE*, 1994, **82**, (9), pp. 1333–1359

[21] HONCHARENKO W., BERTONI H., DAILING J., YEE H.: 'Mechanisms governing UHF propagation on single floors in modern office buildings', *IEEE Trans. Veh. Technol.*, 1992, **41**, (4), pp. 496–504

[22] RAPPAPORT T.S.: 'Wireless communications: principles and practice' (Prentice Hall, 2002, 2nd edn.)

[23] VAUGHAN R., ANDERSEN J.B.: 'Channels, propagation and antennas for mobile communications' (The Institution of Electrical Engineers, 2003)

doi: 10.1049/iet-map:20060305